ORIGINAL PAPER

RJME
Romanian Journal of Morphology & Embryology
http://www.rjme.ro/

MRI differential diagnosis: bone metastases *versus* bone lesions due to malignant hemopathies

ANA MAGDALENA BRATU[1,2)], VICTOR PAUL RAICA[2)], IULIA ALECSANDRA SĂLCIANU[1,2)], CONSTANTIN ZAHARIA[1,2)], VALERIU BOGDAN POPA[1,3)], ANCA ROXANA LUPU[1,4)], VICTORIŢA ŞTEFĂNESCU[5)], CAMELIA-MARIOARA DOBREA[1,6)], GHEORGHE IANA[1,7)], ANDREEA NICOLETA MARINESCU[1,7)]

[1)] *"Carol Davila" University of Medicine and Pharmacy, Bucharest, Romania*

[2)] *Department of Radiology and Medical Imaging, "Colţea" Clinical Hospital, Bucharest, Romania*

[3)] *Department of Radiology and Medical Imaging, "Floreasca" Clinical Emergency Hospital, Bucharest, Romania*

[4)] *Department of Hematology, "Colţea" Clinical Hospital, Bucharest, Romania*

[5)] *Faculty of Medicine and Pharmacy, "Lower Danube" University, Galaţi, Romania; Department of Radiology and Medical Imaging, "Sf. Ioan" Children's Emergency Hospital, Galaţi, Romania*

[6)] *Laboratory of Pathology, Department of Hematology, "Fundeni" Clinical Institute, Bucharest, Romania; Onco Team Diagnostic, Bucharest, Romania*

[7)] *Department of Radiology and Medical Imaging, Clinical Emergency University Hospital, Bucharest, Romania*

Abstract

Bone determinations are usually the first sign of disseminated cancers, whether is a hematological malignancy or other type of neoplasia. The aim of this paper is the possibility of differentiating the bone lesions from hematological malignancies by other malignancies that give bone metastases for the purpose to guide the clinician concerning causality of bone lesions. The research involved a retrospective study, which included 309 cases that were investigated by magnetic resonance imaging (MRI) at a segment of the spine, between 2010 and 2014, from which 137 were diagnosed with a form of hematological neoplasia, and the remaining had another form of cancer. Imaging aspect differs in these two study groups. Bone determinations due to malignant hemopathies (MH) were in general hypointense on T1-weighted sequences, iso- or hyperintense on T2-weighted sequences. On the other hand, bone metastases were hypo- or isointense on T1-weighted sequences, and had no specific signal intensity on T2-weighted sequences. In post-contrast images, all lesions showed contrast enhancement, with some differences. In terms of imagistic aspect, there are certain characteristics that can make a clear differentiation between bone determinations due to MH from the bone metastases, and some are found in the majority of the cases studied.

Keywords: MRI, differential diagnosis, bone metastasis, malignant hemopathies.

Introduction

Bone determinations are often the first evidence of disseminated cancers, the most common types of malignancies that cause bone lesions are breast, prostate and lung cancer [1–5]. Neoplasms of the thyroid and kidneys can also cause them [1–6], but the digestive tract and the neck rarely can determine bone metastasis [6–8].

Hematogenous spread is the most common way of dissemination of malignancies, but bone involvement can occur as a result of direct extension of the primary tumor [9–11].

Lesions occur mainly in the red bone marrow (BM), and therefore the most common sites are the bone segments rich in this type of BM [12, 13]. More than 80% of bone determinations are found at the axial skeleton [6, 14].

Neoplastic effect on bone translates into lytic, sclerotic or mixed bone lesions [15, 16]. Bone metastases are most often osteolytic, but the osteosclerotic lesions may occur in the majority of prostate cancers in 10% of cases of breast cancer and rarely in other types of cancer [17].

The aim of this paper is the possibility of differentiating the bone determinations from hematological malignancies by other malignancies that give bone metastases for the purpose to guide the clinician concerning causality of bone lesions identified with magnetic resonance (MR) investigations.

In case of hematological malignancies, a second neoplastic disease may occur at any time. In this case, it must be established whether bone lesions belong to primary neoplasia, or are due to newly cancer. Also, in some cases of organic cancer can occur a hematological malignancy due to treatment applied, which can determine bone lesions. This requires theirs differential diagnosis.

For this purpose, we analyzed a group of 309 patients who had a form of malignancy with bone determinations. This goal has required the study of bone changes, which were identified on MR images.

Offering a high resolution and an excellent tissue contrast [18], magnetic resonance imaging (MRI) is an ideal tool for detecting bone lesions. MRI is the most reliable method for the investigation of BM, both normal and pathological [19]. MRI is a non-invasive method that allows diagnosis and monitoring the evolution in different malignancies [20].

Patients, Materials and Methods

The research involved a retrospective study, which included 309 cases that were investigated by MRI, at a segment of the spine, between 2010 and 2014. The MRI protocol in the study group implied getting T1- and T2-weighted sequences, and fat suppression sequences in sagittal plane, T2-weighted sequences in coronal and axial plans, followed by T1-weighted sequences post-contrast in all three planes.

In the study were included patients who had developed at least one bone lesion secondary to a neoplastic disease. Demographic data, such as age and gender, were not criteria for inclusion or exclusion from the study, the analysis been based on the specific characters of bone determinations in neoplastic process.

Pathological examination of bone lesions and/or BM biopsies, and immunohistochemistry (IHC) studies established the hematological or non-hematological nature of the proliferation.

The analytical study involved identifying the distinctive characteristics of vertebral lesions found in malignant hemopathies (MH), and those caused by other types of malignancy, followed by comparing the results in order to develop a "pattern" to recognize the underlying neoplastic disease based on the structural, dimensional and numeric features of these bone determinations.

MRI protocol

T1-weighted sequences

In T1-weighted sequences, fat has a short relaxation time, and the water has a long T1 relaxation time (signal intensity is lower than the one of fat) [21].

Therefore, the fatty BM will have high signal intensity, similar to that of the subcutaneous fat tissue. Red BM, on the other hand, due to its composition will determine lower signal intensity than fatty BM, having a signal similar or slightly increase compared to muscles [22].

High signal intensity of fatty BM enables detection of pathological lesions, most having a T1 relaxation time longer than the fat [22].

However, bone lesions can have a T1 relaxation time similar to red BM and identifying them can be difficult by performing only T1-weighted images.

T2-weighted sequences

In T2-weighted sequences, the difference between signal intensity of fat and water is reduced; the result is a poor differentiation between normal BM signal, the fatty marrow and BME [21].

Red BM usually determines a small increase in signal intensity, appearing slightly bright than muscle tissue. Vertebral bodies are darker than the intervertebral discs.

Most bone lesions have a high component of water, and therefore will have a high signal intensity compared to BM, both the fatty and red one. This facilitates the detection of pathological processes in BM [22].

STIR (short-tau inversion recovery) sequence

STIR sequence highlights the difference between the signal from water and fat, by canceling the fat signal [23]. In practice, it is useful to better visualize BM lesions, which will appear bright on a dark background [24].

T1-weighted sequence with intravenous contrast media

In adult, contrast enhancement in normal BM is hardly perceptible visually and easy to differentiate from the one of lesions [25, 26].

Post-contrast and pre-contrast T1-weighted images must be obtained with the same parameters.

Pathological protocol

Biopsies of the tumor lesions (if the tumor was accessible for surgical approach) and/or BM trephine biopsy (if multiple bone lesions were presents) have been performed. For bone marrow biopsy (BMB) is necessary a fragment of at least 1 cm length for a properly histopathological examination. The tissues were fixed in 10% neutral buffered formalin for up to 24 hours, decalcified with disodium ethylenediaminetetraacetate (Na_2EDTA) for 3–4 hours (for BMB) or decalcified with nitric or trichloracetic acid for several days (for large tissues surgically collected). After decalcification and automatic processing, the samples were paraffin embedding; sections of 3 μm thickness were manually cut on the microtome, displayed on slides and standard stained with Hematoxylin–Eosin (HE). A presumptive histopathological diagnosis was established and a panel of antibodies for certainly and differential diagnosis was selected.

IHC protocol

The antibody panel was selected based on histopathological appearances on HE staining. For metastasis, clinical and imaging data (including medical history of the patient) are very important for a first orientation on determining the origin of the proliferation and the antibody panel. IHC staining was carried out on 2 μm thickness paraffin-wax sections using UltraVision Large Volume Detection System (Thermo Fisher Scientific, USA), in accordance with the manufacturer's. The IHC panel was large, and it is revealed in Tables 1 and 2.

Table 1 – ***IHC panel used for most frequently bone metastasis***

Origin	Antibody	Name	Clone	Specificity	Manufacturer	Dilution
Bone metastasis from lung cancer	CK7	Cytokeratin 7	OV-TL 12/30	Positive	Dako, Glostrup, Denmark	1:50
	TTF-1	Thyroid transcription factor-1	SPT24	Positive	Novocastra, Leica, UK	1:100
	Napsin A	Aspartic protease	IP64	Napsin A+ TTF-1+ lung adenocarcinoma	Novocastra, Leica, UK	1:400
	p63		7JUL	Squamous differentiation	Novocastra, Leica, UK	RTU
	CHROMO	Chromogranin	SP12	Neuroendocrine differentiation	Thermo Fisher Scientific, USA	1:800
	SYN	Synaptophysin	27G12		Novocastra, Leica, UK	1:100
	Ki67		MIB-1	Proliferation index	Dako, Glostrup, Denmark	1:100

Origin	Antibody	Name	Clone	Specificity	Manufacturer	Dilution
Bone metastasis from breast cancer	CK7	Cytokeratin 7	OV-TL 12/30	Positive	Dako, Glostrup, Denmark	1:50
	ER	Estrogen receptor	6F11/2	Positive – antiestrogenic therapy	Novocastra, Leica, UK	1:50
	PGR	Progesterone receptor	312	Positive	Novocastra, Leica, UK	1:100
	GCDFP-15	Gross cystic disease fluid protein-15	23A3	Positive	Dako, Glostrup, Denmark	1:30
	E-cadherin	Cell–cell molecular adhesion	NCH-38	Negative in lobular breast carcinoma	Dako, Glostrup, Denmark	1:100
	erbB2	Receptor tyrosine kinase 2	CD11	Her-2/neu gene protein	Cell Marque, Sigma Aldrich, USA	1:100
	Ki67	Proliferation index	MIB-1	Proliferation index	Dako, Glostrup, Denmark	1:100
Bone metastasis from prostatic cancer	PSA	Prostate-specific antigen	ER-PR8	Positive	Dako, Glostrup, Denmark	1:100
	PSMA	Prostate-specific membrane antigen	3E6	Positive	Dako, Glostrup, Denmark	1:50
	AMACR	α-Methylacyl-CoA racemase (P504S)	13H4	Positive	Novocastra, Leica, UK	1:200
Bone metastasis from GI cancer	CK7	Cytokeratin 7	OV-TL 12/30	Positive	Dako, Glostrup, Denmark	1:50
	CK20	Cytokeratin 20	PW31	Negative	Novocastra, Leica, UK	1:100
	CDX2	Caudal-related homeobox transcription factor	EPR2764Y	Positive colonic carcinoma	Cell Marque, Sigma Aldrich, USA	200
	CEA	Carcinoembryonic antigen	CEA-5	Positive GI carcinoma	Dako, Glostrup, Denmark	1:50
Bone metastasis from malignant melanoma	AE1/AE3	Pan-cytokeratin	AE1/AE3	Negative	Novocastra, Leica, UK	1:100
	VIM	Vimentin	V9	Positive	Dako, Glostrup, Denmark	1:50
	S100	S100 protein	Polyclonal	Positive	Dako, Glostrup, Denmark	1:2000
	HMB-45	Melanosome	HMB-45	Positive	Dako, Glostrup, Denmark	1:50
	Melan-A	MART-1	A103	Positive	Dako, Glostrup, Denmark	1:50

IHC: Immunohistochemistry; GI: Gastrointestinal; HMB: Human melanoma black; MART: Melanoma-associated antigen recognized by T-cells; RTU: Ready to use.

Table 2 – ***IHC panel for hematological bone lesions***

Type of tumor	Antibody	Name	Clone	Specificity	Manufacturer	Dilution
Multiple myeloma	CD138	Plasma cells marker	B-A38	Positive	Cell Marque, Sigma Aldrich, USA	1:100
	CD20	B-cells marker	L26	Only 20% positive	Dako, Glostrup, Denmark	1:400
	CD56	NK and cytotoxic cell marker	M7304	~80% positive	Dako, Glostrup, Denmark	1:50
	Kappa	Kappa light chain		Clonal report	Novocastra, Leica, UK	1:2000
	Lambda	Lambda light chain			Novocastra, Leica, UK	1:300
Malignant lymphomas	CD45	Common leukocyte antigen	X16/99	Usually positive	Novocastra, Leica, UK	1:100
	CD20	B-cells marker	L26	B-cell lymphoma	Dako, Glostrup, Denmark	1:400
	CD3	T-cells marker	LN10	T-cell lymphoma	Novocastra, Leica, UK	1:300
	CD10	Germinal-centre marker	56C6	B-cell lymphoma (FL, DLBCL, Burkitt); AITL	Novocastra, Leica, UK	1:50
	BCL6	Germinal-centre marker	LN22	B-cell lymphoma (FL, DLBCL, Burkitt); AITL	Novocastra, Leica, UK	1:50
	MUM-1	Multiple myeloma oncogene-1	EAU32	Activated DLBCL	Novocastra, Leica, UK	1:50
	CD30	Activated lymphocyte	HRS4	Hodgkin's lymphomas; ALCL	Thermo Fisher Scientific, USA	1:30
	Cyclin D1		SP4	MCL	Cell Marque, Sigma Aldrich, USA	1:50
	CD5	T-cells marker	SP19	T-cell lymphoma; aberrant expression in B-cell lymphoma (MCL, B-SLL/B-CLL)	Cell Marque, Sigma Aldrich, USA	1:50
	CD23	Follicular dendritic cells	1B12	Aberrant expression in B-SLL/B-CLL	Novocastra, Leica, UK	1:50
	PD1	Follicular helper T-cells	NAT105	AITL	Cell Marque, Sigma Aldrich, USA	1:50
	CD25	Interleukin-2 receptor	7G7/B6	HCL, ATLL	Novocastra, Leica, UK	1:50
	Ki67		MIB-1	Proliferation index	Dako, Glostrup, Denmark	1:100

IHC: Immunohistochemistry; NK: Natural killer; FL: Follicular lymphoma; DLBCL: Diffuse large B-cell lymphoma; AITL: Angioimmunoblastic T-cell lymphoma; ALCL: Anaplastic large cell lymphoma; MCL: Mantle cell lymphoma; B-SLL/B-CLL: B-small lymphocyte lymphoma/chronic lymphocyte leukemia; HCL: Hairy-cell leukemia; ATLL: Adult T-cell leukemia/lymphoma.

Results

Three hundred and nine patients were investigated by MRI at a segment of spine. All developed at least one bone lesion consecutive to a malignant disease.

Of the 309 patients, 44.33% were diagnosed with a form of hematological neoplasia, and the 55.66% remaining had another form of cancer (Table 3). The group of patients with hematological malignancies comprised a total of 73 cases with multiple myeloma (MM) (Figure 1), 47 with lymphoma (Figure 2), the remaining 17 being diagnosed with leukemia (Figure 3). The group of patients with other forms of cancer was more heterogeneous (Figures 4–7), being revealed in Table 3.

In the group of patients with bone lesions in the spine due to hematological malignancies, it was observed that only 5.83% of the lesions also occur in the vertebral pedicles (Figure 8A), being represented by two cases of lymphoma and six with MM. None of the cases of leukemia presented lesions on the pedicles.

On the other hand, in case of bone metastasis caused by other types of malignancy was found that lesions in pedicles (Figure 8B) are present in a rate of 26.74% (Table 4). However, not in all cases, as shown in Table 4.

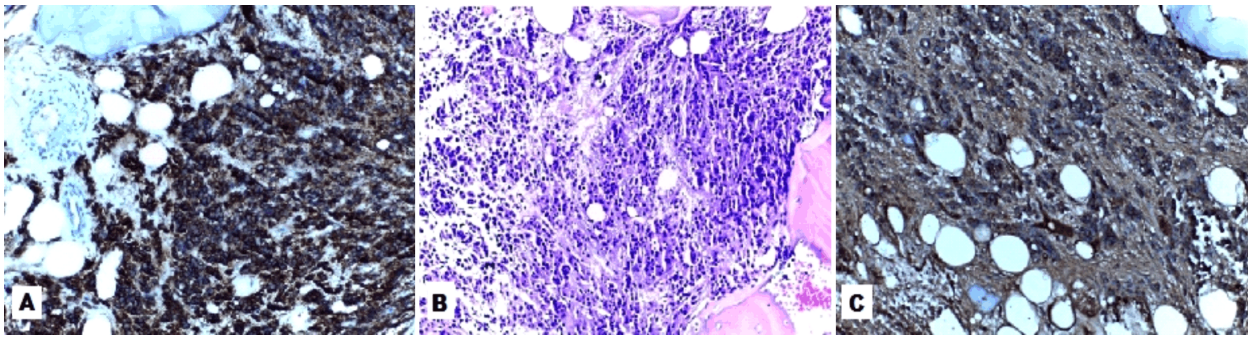

Figure 1 – ***Multiple myeloma: (A) Tumor proliferation is CD138 positive (Anti-CD138 antibody immunostaining, ×200); (B) HE staining, ×200; (C) Lambda light chain restriction (Anti-lambda light chain antibody immunostaining, ×200).***

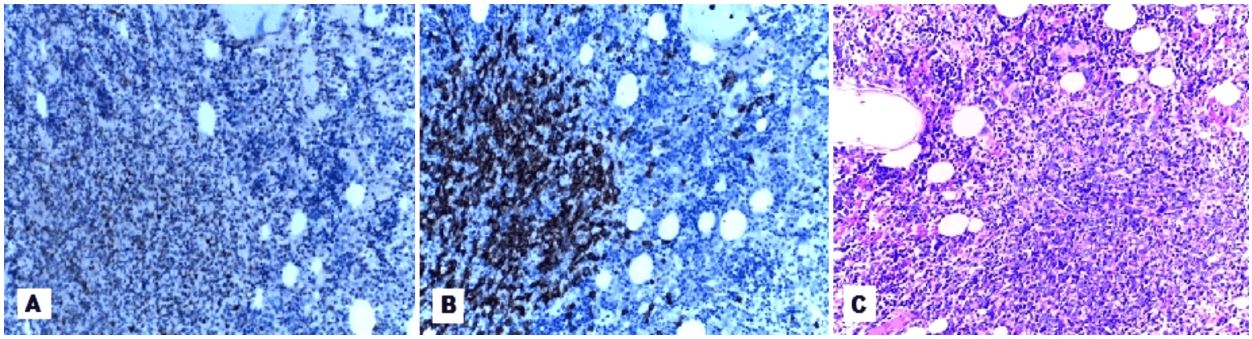

Figure 2 – ***Bone marrow trephine biopsy infiltration of follicular lymphoma: (A) Malignant B-cells express BCL6, follicular B-cells marker (Anti-BCL6 antibody immunostaining, ×200); (B) Tumor lymphoma infiltrate with CD20-positive B-cells (Anti-CD20 antibody immunostaining, ×200); (C) Follicular lymphoma (HE staining, ×200).***

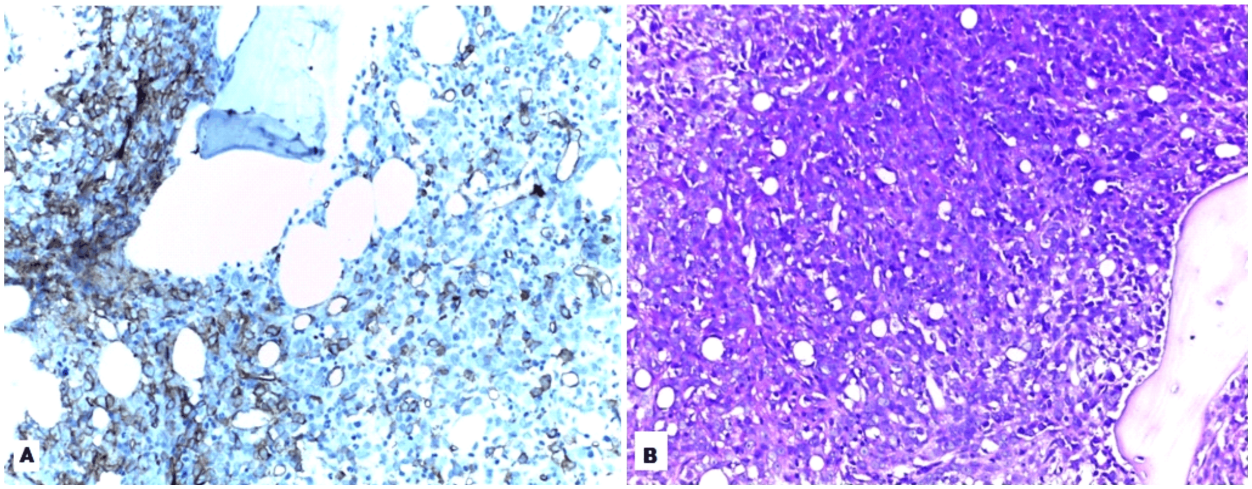

Figure 3 – ***Bone marrow trephine biopsy – acute myeloid leukemia: (A) Tumor blasts cells are CD34 positive (Anti-CD34 antibody immunostaining, ×200); (B) HE staining, ×200.***

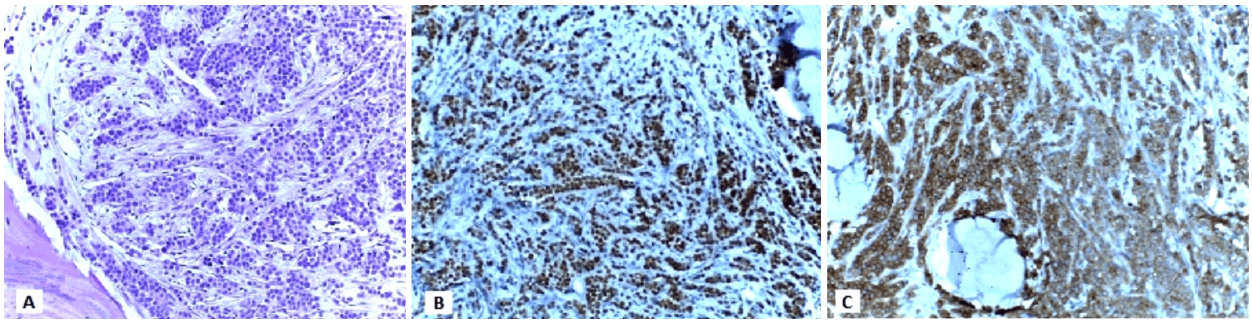

Figure 4 – ***Bone metastasis of breast carcinoma: (A) HE staining, ×200; (B) Tumor cells are estrogen receptor (ER) positive (Anti-ER antibody immunostaining, ×200); (C) Strong complete membrane staining for Her-2/neu in >10% of cancer cells (3+) (Anti-Her-2/neu antibody immunostaining, ×200).***

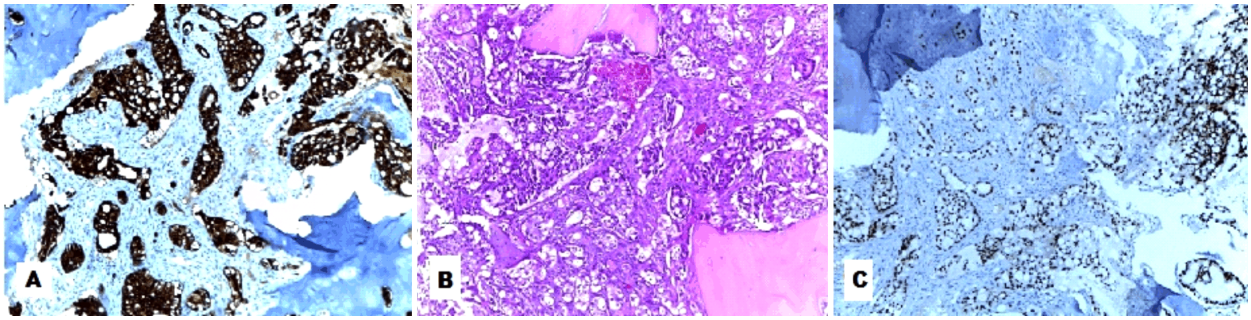

Figure 5 – ***Bone metastasis of lung adenocarcinoma: (A) Cytokeratin 7 (CK7) positive in malignant proliferation (Anti-CK7 antibody immunostaining, ×200); (B) HE staining, ×200; (C) Tumor cells are thyroid transcription factor-1 (TTF-1) positive (Anti-TTF-1 antibody immunostaining, ×100).***

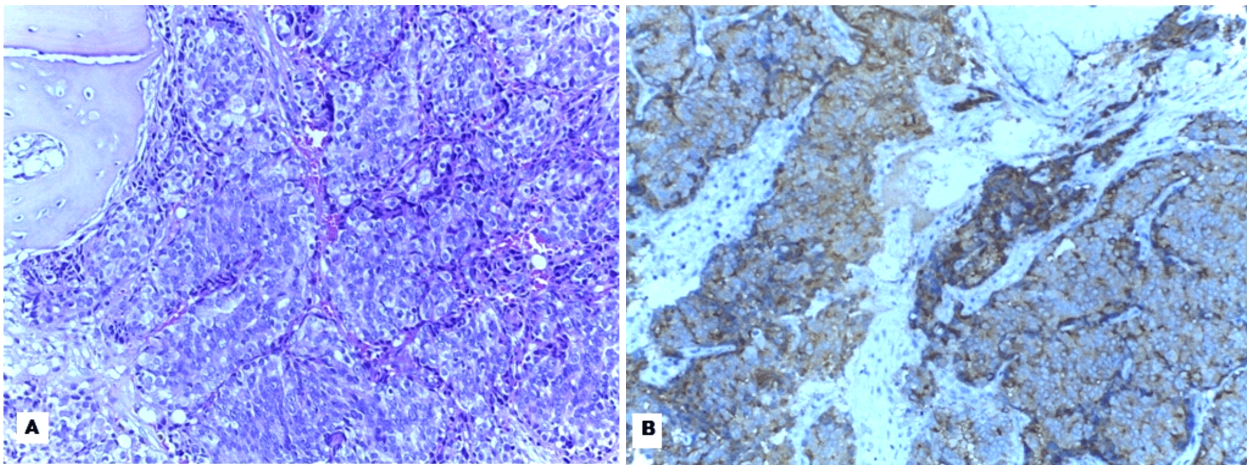

Figure 6 – ***Bone metastasis of prostate carcinoma: (A) HE staining, ×200; (B) Tumor cells expressed prostate-specific membrane antigen (PSMA) (Anti-PSMA antibody immunostaining, ×200).***

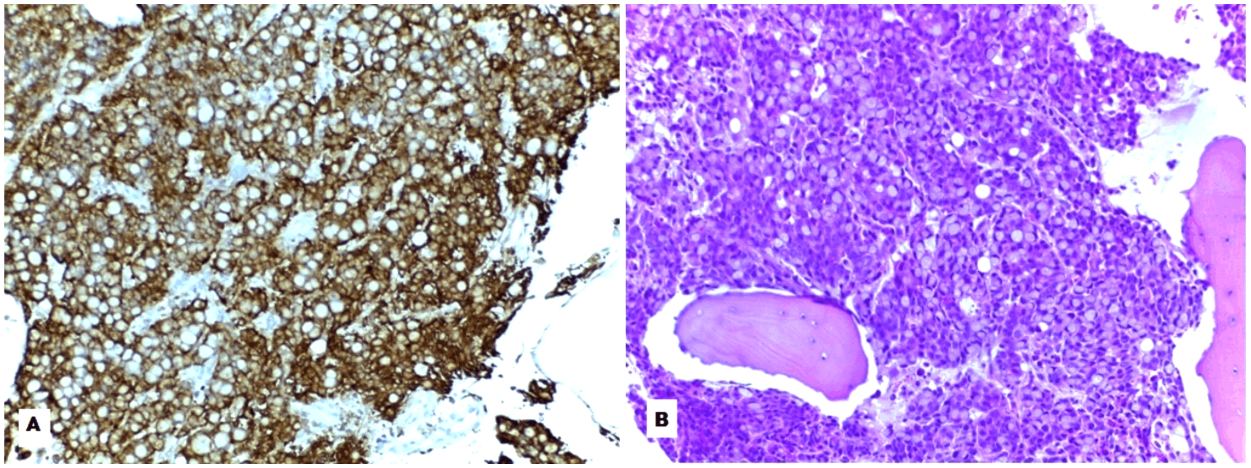

Figure 7 – ***Bone metastasis of gastric signet ring cells carcinoma: (A) Tumor cells are carcinoembryonic antigen (CEA) positive (Anti-CEA antibody immunostaining, ×200); (B) HE staining, ×200.***

Table 3 – ***Numerical distribution of cases with other form of malignancies than hematological malignancies***

Malignancy	No. of cases
Pancreatic cancer	4
Breast cancer	43
Lung cancer	76
Thyroid cancer	7
Prostate cancer	14
Bladder cancer	5
Kidney cancer	7
Ovarian cancer	3
GI tract cancer	6
Malignant melanoma	5
Neck SCC	2

GI: Gastrointestinal; SCC: Squamous cell carcinoma.

Depending on the signal of bone lesions identified on MR images, it was observed that all, which were found in hematological patients, had a lytic appearance, translated in low signal intensity on T1-weighted images, iso- or hypersignal intensity on T2-weighted images, and in hypersignal on STIR sequences.

Bone lesions identified in patients with neoplasia, other than hematological malignancies, were lytic in majority (65.69%). It were observed also sclerotic lesions in 9.3% of cases, and mixed in 13.37% of patients (Table 5). Withal, there have been identified bone metastases that had sclerotic marginal rim in 11.62% of patients (Table 5). This aspect has not been identified in the group of patients with hematological malignancies.

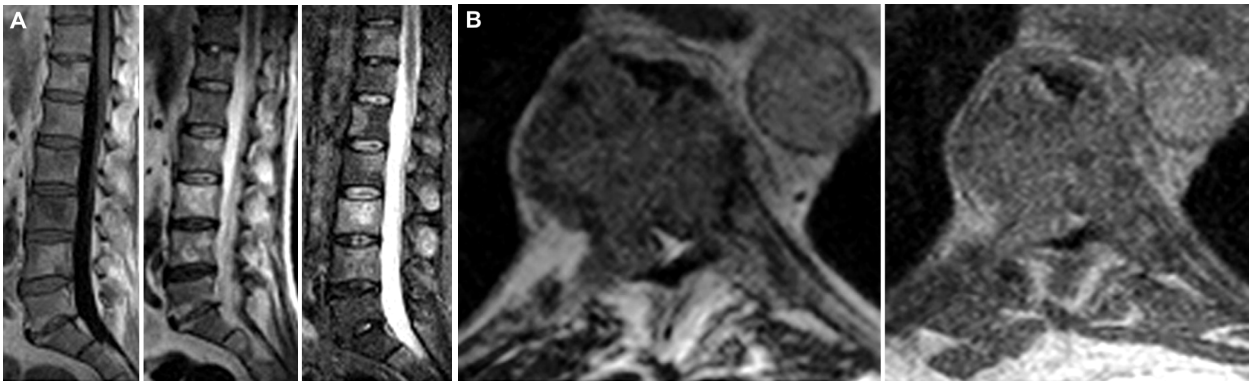

Figure 8 – ***(A) Lumbar spine MRI: T1 and T2-weighted sequences, and STIR sequence – bone determinations which affect only the vertebral bodies at a patient with MH; (B) Thoracic spine MRI: T1-weighted sequence, pre- and post-contrast – metastases on vertebral body and right pedicle. MRI: Magnetic resonance imaging; STIR: Short-tau inversion recovery; MH: Malignant hemopathy.***

Table 4 – ***Distribution of cases with metastases in the pedicles***

Malignancy	No. of cases with pedicle involvement
Pancreatic cancer	1
Breast cancer	12
Lung cancer	21
Thyroid cancer	2
Prostate cancer	5
Bladder cancer	1
Kidney cancer	3
Ovarian cancer	0
GI tract cancer	1
Malignant melanoma	0
Neck SCC	0

GI: Gastrointestinal; SCC: Squamous cell carcinoma.

Table 5 – ***Distribution of cases with metastases depending on the type of structure***

Malignancy	No. of cases			
	Lytic	*Sclerotic*	*Mixed*	*Marginal rim*
Pancreatic cancer	4	0	0	0
Breast cancer	32	0	7	4
Lung cancer	51	0	16	9
Thyroid cancer	7	0	0	0
Prostate cancer	0	8	0	6
Bladder cancer	0	5	0	0
Kidney cancer	6	0	0	1
Ovarian cancer	0	3	0	0
GI tract cancer	6	0	0	0
Malignant melanoma	5	0	0	0
Neck SCC	2	0	0	0

GI: Gastrointestinal; SCC: Squamous cell carcinoma.

In post-contrast T1-weighted sequences, moderate enhancement was identified in 88 patients who presented a form of hematological neoplasia (Figure 9A), representing the majority in this study. Low contrast uptake was seen in 45 patients and the remaining four showed an intense contrast uptake. In the group of patients with another form of malignancy were identified 36 cases that showed a heterogeneous contrast enhancement (Figure 9B). Intense contrast uptake was seen in the majority of cases (100 patients), followed by moderate contrast enhancement (32 cases), and low contrast uptake has been identified in four cases. Distribution of cases depending on the type of contrast enhancement is revealed in Table 6.

On the MRI images was noticed that hematological bone lesions were associated with bone marrow edema (BME) in a percentage of 43.8% (Figure 10A), while bone metastases (Figure 10B) in a rate of only 9.3% (Table 7).

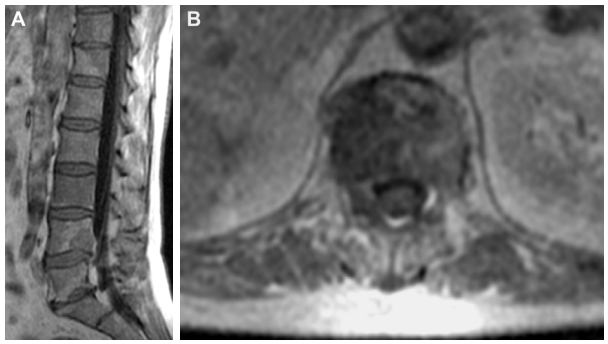

Figure 9 – ***(A) Lumbar spine MRI: Post-contrast T1-weighted sequence – homogeneous enhancement of vertebral lesions at a patient with MH; (B) Lumbar spine MRI: Post-contrast T1-weighted sequence – heterogeneous enhancement of vertebral metastasis. MRI: Magnetic resonance imaging; MH: Malignant hemopathy.***

Bone lesions from hematological malignancies determined disruption of cortical bone in a minority of cases of only 3.65%, being represented by one case with MM and four patients who had been diagnosed with lymphoma; in the remaining cases of MH the cortical bone was unimpaired (Figure 11A). On the other hand, metastases showed cortical disruption in a majority ratio of 56.97% (Figure 11B). It has also been observed that metastases can determine thinning of cortical bone, in a percentage of 18.6% (Table 8). In the study group of patients with MH we have not identified any bone lesion which determines that kind of change in the cortical bone.

Depending on the number of lesions identified on a bone segment, it was observed that all cases of hematological malignancies had at least three lesions at a segment of spine. In the group of patients with other forms of neoplasm, was noticed that the rate of solitary lesion showed a ratio of 9.88% of cases, and 9.3% of patients with metastases had between one and three lesions on one bone segment (Table 9).

In terms of size, we observed that hematological bone lesions are mostly less than 1 cm (54.01%), lesions greater than 2 cm representing a low ratio of 5.11%. Bone metastases, however, are found in most cases (70.93%) with size larger than 2 cm (Table 10).

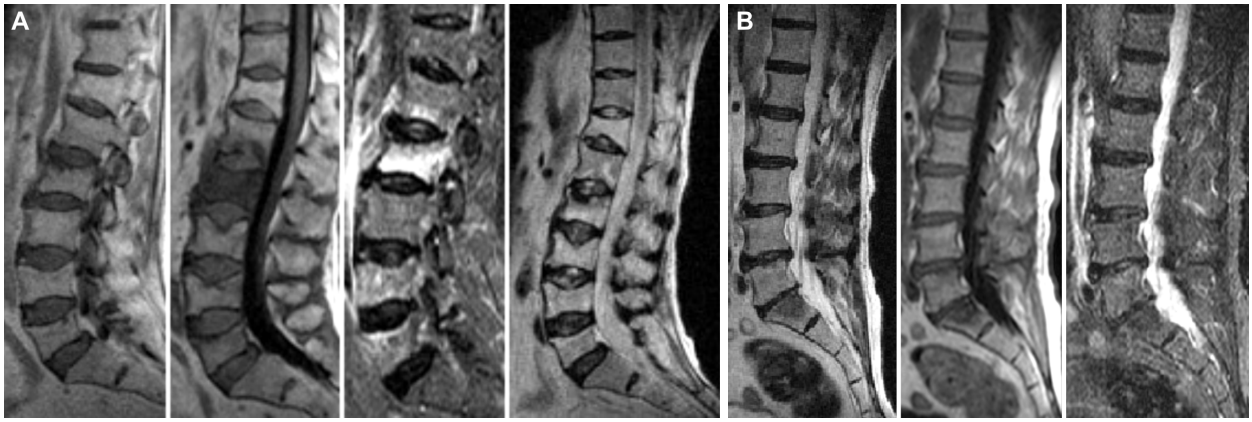

Figure 10 – ***Lumbar spine MRI: (A) T2- and T1-weighted sequences, STIR sequence, and T1 post-contrast: BME on a patient with MH; (B) T2- and T1-weighted sequences, and STIR sequence: Bone metastases without BME. MRI: Magnetic resonance imaging; STIR: Short-tau inversion recovery; BME: Bone marrow edema; MH: Malignant hemopathy.***

Figure 11 – ***(A) Cervical spine MRI: T1-weighted sequence, pre- and post-contrast – lytic lesions on a patient with MH, with unimpaired cortical bone; (B) Thoracic spine MRI: T1- and T2-weighted sequences, STIR sequence, and T1 post-contrast – tumor mass with disruption of cortical bone, and extension in the spinal canal on a patient with bone metastases. MRI: Magnetic resonance imaging; MH: Malignant hemopathy; STIR: Short-tau inversion recovery.***

Table 6 – ***Distribution of cases depending on the type of contrast enhancement***

Malignancy	No. of cases			
	Low	*Moderate*	*Intense*	*Heterogeneous*
Multiple myeloma	29	44	0	0
Lymphoma	14	29	4	0
Leukemia	2	15	0	0
Pancreatic cancer	0	0	4	0
Breast cancer	2	19	16	6
Lung cancer	2	4	46	24
Thyroid cancer	0	0	6	1
Prostate cancer	0	3	11	0
Bladder cancer	0	0	5	0
Kidney cancer	0	0	5	2
Ovarian cancer	0	0	1	2
GI tract cancer	0	5	0	1
Malignant melanoma	0	1	4	0
Neck SCC	0	0	2	0

GI: Gastrointestinal; SCC: Squamous cell carcinoma.

Table 7 – ***Distribution of cases with spinal lesions associated with BME***

Malignancy	No. of cases with BME
Multiple myeloma	32
Lymphoma	21
Leukemia	7
Pancreatic cancer	0
Breast cancer	4
Lung cancer	8
Thyroid cancer	1
Prostate cancer	2
Bladder cancer	0
Kidney cancer	1
Ovarian cancer	0
GI tract cancer	0
Malignant melanoma	0
Neck SCC	0

BME: Bone marrow edema; GI: Gastrointestinal; SCC: Squamous cell carcinoma.

Table 8 – ***Distribution of cases with metastases that determine changes in cortical bone***

Malignancy	No. of cases that cause disruption of cortical bone	No. of cases that cause thinning of cortical bone
Pancreatic cancer	2	0
Breast cancer	26	11
Lung cancer	48	16
Thyroid cancer	4	1
Prostate cancer	9	3
Bladder cancer	2	0
Kidney cancer	4	1
Ovarian cancer	0	0
GI tract cancer	2	0
Malignant melanoma	1	0
Neck SCC	0	0

GI: Gastrointestinal; SCC: Squamous cell carcinoma.

Table 9 – ***Distribution of cases depending on the number of lesions identified on a vertebral segment***

Malignancy	No. of cases		
	Unique	*1–3 lesions*	*>3 lesions*
Multiple myeloma	0	0	73
Lymphoma	0	0	47
Leukemia	0	0	17
Pancreatic cancer	0	0	4
Breast cancer	2	4	37
Lung cancer	14	11	51
Thyroid cancer	0	1	6
Prostate cancer	0	0	14
Bladder cancer	0	0	5
Kidney cancer	1	0	6
Ovarian cancer	0	0	3
GI tract cancer	0	0	6
Malignant melanoma	0	0	5
Neck SCC	0	0	2

GI: Gastrointestinal; SCC: Squamous cell carcinoma.

Table 10 – ***Distribution of cases depending on the size of lesions***

Malignancy	No. of cases		
	<1 cm	*1–2 cm*	*>2 cm*
Multiple myeloma	41	30	2
Lymphoma	23	19	5
Leukemia	10	7	0
Pancreatic cancer	0	0	4
Breast cancer	7	11	25
Lung cancer	3	4	69
Thyroid cancer	0	3	4
Prostate cancer	0	5	9
Bladder cancer	0	1	4
Kidney cancer	0	5	2
Ovarian cancer	0	0	3
GI tract cancer	4	2	0
Malignant melanoma	0	3	2
Neck SCC	2	0	0

GI: Gastrointestinal; SCC: Squamous cell carcinoma.

Discussion

In a patient with neoplastic disease, MRI is usually performed to detect metastatic disease in the spine, spinal cord compression and also on the nerve roots.

MRI is a non-invasive method and brings the most information about the pathological entity [19]. MRI can detect early malignant bone lesion, before the existence of cortical destruction or reactive processes [18, 27].

Spinal metastases occur in 10% of all patients with malignant tumors and represents 39% of the total bone metastases. Detecting metastatic disease in the vertebral bodies is important for appropriate treatment of patients with malignant disease. In addition, bone metastasis can determine cord compression or on the nerve roots, causing neurological deficits that may significantly alter disease course and treatment of a patient [20].

The vertebral body, which contains most of the red marrow, is more likely to develop metastases than other segments of the vertebra. Withal, the vertebral pedicle is composed mainly from cortical bone, and contains practically no BM [28].

In the study group it was observed that bone lesions due to hematological malignancies tend to be localized mainly in the vertebral body, and only very few cases showed involvement of vertebral pedicles. In agreement with this, Kumar *et al.* [29] and Tosi [30] stated that lesions in MM are located rarely in pedicles. The subgroup of patients with leukemia showed no bone lesions to the pedicles, which we consider not to be due to the small number of patients with this hematological neoplasia but rather the fact that the pedicles are an atypical location of leukemic bone lesions.

Instead, bone metastases are located in the pedicles in a significant percentage in the study group. Kim *et al.* [31] stated that pedicle involvement is well-known phenomenon of metastatic tumors. Shah & Salzman [32] added that blastic metastases tend to destroy the posterior cortex and involve the pedicle. Also, lytic lesions may involve the posterior cortex with destruction of it and pedicle.

In their group of 45 patients with 95 vertebral metastases, Algra *et al.* [33] specifies that pedicles had lesions in 53 vertebrae and was never seen without the involvement of the posterior part of the vertebra; this suggests that the invasion and destruction of the pedicle through the metastatic process occurs only through the vertebral body.

On the other hand, more than 90% of the cases described in the study by Jacobson *et al.* [34] showed the involvement of the pedicles; in our study group only 17.47% indicate lesions in pedicles, from which 85.18% were metastases; it is assumed that the study group analyzed by Jacobson *et al.* included patients in an advanced stage of metastatic disease.

Maccauro *et al.* [35] suggests that the original location of metastases in the vertebra is in the posterior part of the body. Lesions in pedicles occur only in combination with vertebral body involvement [33].

On the other hand, other authors [36] state that the posterior part of the vertebral body is preferentially involved.

Even-Sapir [18] and Roodman [37] affirm that lytic form, sclerotic and mixed type of bone metastases is different depending on underlying neoplasia. Lytic lesions can be seen in almost all tumor types [17, 38].

Primary tumors, which typically have lytic spinal metastases, are breast, lung, kidney, thyroid, oropharyngeal, melanoma, adrenal, and uterus. Breast and lung cancer may also show mixed lytic and sclerotic lesions, which are seen with ovarian, testicular, and cervical carcinomas. Prostate, bladder, nasopharynx, medulloblastoma, neuroblastoma, and bronchial carcinoid primaries commonly have blastic-appearing spinal metastases [32]. The areas of sclerosis may be nodular or mottled in appearance, and have hypointensity on all MR sequences.

On the images obtained by MRI, bone lesions due to hematological malignancies presented hyposignal in T1-weighted sequences. On T2-weighted sequences, most of them showed hypersignal, or they were isointense. The sequence with fat suppression highlighted all bone lesions as hyperintense. Post-administration of gadolinium is observed homogenous enhancement, whether it was low, moderate or intense. This aspect is specific for lytic lesions.

Consistent with data obtained in our study group, typical bone lesions from hematological malignancies described in the literature shows a low signal intensity on T1-weighted images, are hyperintense on T2-weighted and STIR sequences [39–41], and enhance homogeneous on post-gadolinium T1-weighted images [39–42]. However, MRI findings are usually non-specific [39–41].

In a study by Daffner *et al.* [43], which included a total of 80 patients with various malignancies, 30 of them were diagnosed with MM. The authors noted that the BM showed low signal intensity on T1-weighted images in 80% of patients with metastases, and in all patients with myeloma.

In the present study, bone metastases were lytic, sclerotic or mixed, as were presented in the Table 5, with hypo- or isointensity on T1-weighted sequences, without specific signal in T2-weighted sequences. In STIR sequence, lesions were hypo- or hyperintense. On post-contrast T1-weighted images was observed that bone metastases may present heterogeneous enhancement (1/5 of cases), and it is intense in more than half of cases.

Normal BM in adults is hyperintense on T1-weighted images [27, 44], whereas the metastases show a low signal intensity, reflecting the replacement of fat by tumor cells [18, 44–46].

Withal, bone metastases have longer T1 and T2 relaxation time than normal BM and enhance after administration of contrast agent [18].

In literature is presented that metastases shows a higher signal intensity than normal BM on T2-weighted images due to high water content [27, 47], but they may also be isointense with normal BM [44]. In sclerotic bone lesions, such as those from prostate carcinoma, metastases may present low signal intensity on both T1- and T2-weighted images, because only few tumor cells are present between sclerotic trabeculae [46].

In fat suppression sequences, metastases demonstrate heterogeneous or high signal intensity and can thus be easily differentiated from BM [44, 48].

Post-contrast, bone lesions enhance in varying degrees, depending on the vascularization of underlying pathological process [42].

In their study, An *et al.* [49] have identified five contrast enhancement patterns, which were classified as: homogeneous, heterogeneous, non-enhancing, peripheral rim enhancement, and "worms-in-bag" aspect. The pattern "worms-in-bag" was named due to the appearance of many curvilinear structures, which show an intense contrast uptake into a tumor mass with moderate enhancement. It was observed that the metastases had heterogeneous contrast uptake in 31.4% cases.

In terms of structure, it was noticed that hematological bone lesions are homogeneous, showed no surrounding rim, and did not cause thinning of cortical bone. In a few cases (n=5), had broken the cortical bone, extending into neighboring tissues.

In the literature, we found no published papers that showed hematological bone lesions that may cause interruption of cortical bone with loco-regional invasion.

Bone metastases showed a sclerotic rim in about 1/6 of cases. Invasive character is demonstrated by disruption of cortical bone in over half of cases. Also, it was observed that these can cause cortical thinning. We believe that we did not identified metastases which damage the cortical bone in patients with ovarian cancer not because it is a cancer that cannot cause it, but rather because of the small number of cases currently in the study group.

A metastatic lesion was considered to have well defined margins if is clearly separated from adjacent normal tissue and has a smooth, regular contour. If metastasis does not meet these criteria, or involves an entire vertebral body, the delineation was considered ill-defined [49].

An *et al.* [49] performed a study on a group that included 169 patients with various malignancies, except MH. They noted that bone metastases shows well-defined edges in 65.7% of cases, and the remaining 34.3% were invasive bone tumor masses.

Several authors [45–47] state that metastases often, but not always, can have a hyperintense T2 rim ("halo" sign). This "halo" sign may be useful in assessment of sclerotic small metastases that might otherwise be mistaken for osteoma [46].

BME is a non-specific MRI modification due to osteoporosis, trauma [50], infections [44], ischemia [6, 17] or neoplasia [51, 52], and is usually focal, consisting of a non-specific increase of water content in the BM [53].

On MRI images is identified as areas of hyposignal on T1-weighted sequences, high signal intensity on T2-weighted and STIR sequences, and intense enhancement on post-contrast T1-weighted sequences [2, 54, 55].

The semiological characters of BME do not allow primary specific diagnostic differentiation between of the two main groups discussed in the study, the differentiation between the two groups of pathology is possible only through direct cooperation between the radiologist, which precisely locates the lesion and the pathologist, who can specify the exact nature of the lesion. They are more specific when monitoring lesions under treatment in hematological malignancies [21] when it was described the presence of diffuse or focal areas of BME [14, 56].

Chemotherapy induces BME through changes in the structure and vascularization of BM [2, 56]. In early stages of treatment, sinusoidal capillaries within BM become dilated and hyperpermeable, leading to edema [14, 21].

Both by MRI and by histopathological exam, acute and chronic changes induced by radiotherapy have been well described [21, 46]. In the acute phase, cell depletion, BME, vascular congestion, and hemorrhage occur in the first hours and days. In 1–2 weeks, can be observed an increase in MR signal intensity in T2-weighted images and STIR, which is considered to be due to the reduction in cellularity, and BME [55, 57].

In the hematological patients group, it was observed that bone lesions associated with BME in over half of cases. On the other hand, bone metastases associated BME in 16 cases only. However, James *et al.* [58] and Starr *et al.* [59] stated that it is not uncommon to identify surrounding edema in case of bone metastases.

In terms of number of lesions within a segment of the spine, it has been noticed that bone lesions in hematological malignancies are multiple in all cases, defining the disseminated character of the diseases. In patients with bone metastases were identified also multiple lesions (over 3), but there were also cases of unique lesions or at the most two.

Consistent with this, Even-Sapir [18] specifies in his article that MH can cause solitary bone lesions, but more often they are multiple.

Solitary bone metastases are rare, according to Nielsen *et al.* [17], except in patients with renal carcinoma or neuroblastoma, in which 5–10% of patients may have unique bone lesions [1, 3]. In our study, the subgroup of kidney cancer presented unique metastases in 1/7 of cases. Then again, Bhandari & Jain [60] assert that patients with neck cancer may develop solitary or multiple bone metastases, but in our study, all the patients with this type of neoplasia developed more than three lesions at the level of a vertebral segment.

An *et al.* [49] states that the aggressiveness of vertebral metastases may be reflected by the number of lesions found in a patient. In their study, patients had on average at least five bone lesions, and to a lesser proportion between two and five lesions/case.

On the other hand, Khaw *et al.* [61] presented a different frequency of cases with multiple bone lesions; only 43% of the cases studied had multiple involvements.

Regarding dimensional character we identified in the study group that bone lesions due to MH rarely have size over 2 cm, being in general less than 1 cm. In contrast, bone metastases are predominantly large, more than 2 cm, regardless of their underlying neoplasm.

In the study conducted by An *et al.* [49], out of 169 bone metastases identified, 42 lesions involved the entire vertebral body, and eight lesions invaded the posterior vertebral elements without form an expansive tumor mass. The other 119 metastases had sizes between 0.2 and 8 cm, with an average of 1.4 cm.

In another study [62] is mentioned that lesions with sizes of 5 cm or more are diagnosed using MRI in 100% cases, the specificity of the method being lower in metastases with sizes less than 1 cm. Of the 42 metastases confirmed by MRI, four lesions were less than 1 cm, 23 between 1 and 5 cm, and 15 had more than 5 cm in diameter.

Conclusions

Signal intensity changes on MR images do not differentiate between bone metastases and bone determinations due to MH. The exception is the presence of circumscribed lesions, isointense on T1-weighted sequences, with hyposignal intensity in T2-weighted, and STIR sequences, that raise suspicion of bone metastases, ruling out a possible diagnosis of bone lesions from hematological malignancies. This is reinforced by heterogeneous contrast enhancement, which in our study is not present in case of hematological malignancies. The presence of bone lesions, with heterogeneous structure, that causes thinning or interruption

of cortical bone, orientate toward diagnosis of bone metastases. Even if disruption of cortical bone cannot completely exclude MH, leukemia is totally excluded in this situation. The existence of circumscribed lesions, no more than three on a bone segment, associated with involvement of vertebral pedicles, with little, or no surrounding BME, will favor the diagnosis of bone metastases. The detection of bone lesions, measuring up to 2 cm, with surrounding BME, raise suspicion of bone lesions due to hematological malignancies. Bone lesions with diameter less than 1 cm can raise the suspicion of bone lesions from MM.

Conflict of interests

The authors declare that they have no conflict of interests.

Author contribution

All authors of this research paper have directly participated in the planning, execution, or analysis of this study, and also all authors of this paper have read and approved the final version submitted.

References

[1] Stoll BA. Natural history, prognosis, and staging of bone metastases. In: Stoll BA, Parbhoo S (eds). Bone metastases: monitoring and treatment. Raven Press, New York, 1983, 1–20.

[2] Mauch PM, Drew MA. Treatment of metastatic cancer to bone. In: DeVita VT Jr, Hellman S, Rosenberg SA (eds). Cancer, principles & practice of oncology. 2nd edition, Lippincott Williams & Wilkins, Philadelphia, 1985, 2132–2141.

[3] Lote K, Walløe A, Bjersand A. Bone metastasis. Prognosis, diagnosis and treatment. Acta Radiol Oncol, 1986, 25(4–6): 227–232.

[4] Malawer MM, Delaney TF. Treatment of metastatic cancer to bone. In: DeVita VT Jr, Hellman S, Rosenberg SA (eds). Cancer, principles & practice of oncology. 3rd edition, Lippincott Williams & Wilkins, Philadelphia, 1989, 2298–2317.

[5] Patanaphan V, Salazar OM, Risco R. Breast cancer: metastatic patterns and their prognosis. South Med J, 1988, 81(9): 1109–1112.

[6] Coleman RE. Clinical features of metastatic bone disease and risk of skeletal morbidity. Clin Cancer Res, 2006, 12(20 Pt 2): 6243s–6249s.

[7] Kapoor A, Kalwar A, Narayan S, Kumar N, Singhal MK, Kumar HS. Analysis of bone metastasis in head and neck squamous cell carcinoma: experience of a regional cancer center. Clin Cancer Investig J, 2015, 4(2):206–210.

[8] Bhandari V. Incidence of bone metastasis in carcinoma buccal mucosa. Indian J Med Paediatr Oncol, 2016, 37(2):70–73.

[9] Carter RL. Patterns and mechanisms of bone metastases. J R Soc Med, 1985, 78(Suppl 9):2–6.

[10] Carter RL. Patterns and mechanisms of localized bone invasion by tumors: studies with squamous carcinomas of the head and neck. Critical Rev Clin Lab Sci, 1985, 22(3): 275–315.

[11] Gowen GF, Desuto-Nagy G. The incidence and sites of distant metastases in head and neck carcinoma. Surg Gynecol Obstet, 1963, 116:603–607.

[12] Jacobs SC. Spread of prostatic cancer to bone. Urology, 1983, 21(4):337–344.

[13] Berrettoni BA, Carter JR. Mechanisms of cancer metastasis to bone. J Bone Joint Surg Am, 1986, 68(2):308–312.

[14] Miller F, Whitehill R. Carcinoma of the breast metastatic to the skeleton. Clin Orthop Relat Res, 1984, (184):121–127.

[15] Paterson AH. Bone metastases in breast cancer, prostate cancer and myeloma. Bone, 1987, 8(Suppl 1):S17–S22.

[16] Mundy GR. Bone resorption and turnover in health and disease. Bone, 1987, 8(Suppl 1):S9–S16.

[17] Nielsen OS, Munro AJ, Tannock IF. Bone metastases: pathophysiology and management policy. J Clin Oncol, 1991, 9(3): 509–524.

[18] Even-Sapir E. Imaging of malignant bone involvement by morphologic, scintigraphic, and hybrid modalities. J Nucl Med, 2005, 46(8):1356–1367.

[19] Hwang S, Panicek DM. Magnetic resonance imaging of bone marrow in oncology, Part 1. Skeletal Radiol, 2007, 36(10): 913–920.

[20] Mehta RC, Marks MP, Hinks RS, Glover GH, Enzmann DR. MR evaluation of vertebral metastases: T1-weighted, short-inversion-time inversion recovery, fast spin-echo, and inversion-recovery fast spin-echo sequences. AJNR Am J Neuroradiol, 1995, 16(2):281–288.

[21] Sălcianu IA, Bratu AM, Bondari S, Dobrea C, Coliţă A, Zaharia C, Bondari D. Bone marrow edema – premonitory sign in malignant hemopathies or nonspecific change? Rom J Morphol Embryol, 2014, 55(3 Suppl):1079–1084.

[22] Vogler JB 3rd, Murphy WA. Bone marrow imaging. Radiology, 1988, 168(3):679–693.

[23] Mirowitz SA, Apicella P, Reinus WR, Hammerman AM. MR imaging of bone marrow lesions: relative conspicuousness on T1-weighted, fat-suppressed T2-weighted, and STIR images. AJR Am J Roentgenol, 1994, 162(1):215–221.

[24] Bydder GM, Young IR. MR imaging: clinical use of the inversion recovery sequence. J Comput Assist Tomogr, 1985, 9(4):659–675.

[25] Breger RK, Williams AL, Daniels DL, Czervionke LF, Mark LP, Haughton VM, Papke RA, Coffer M. Contrast enhancement in spinal MR imaging. AJR Am J Roentgenol, 1989, 153(2): 387–391.

[26] Sze G, Bravo S, Baierl P, Shimkin PM. Developing spinal column: gadolinium-enhanced MR imaging. Radiology, 1991, 180(2):497–502.

[27] Rybak LD, Rosenthal DI. Radiological imaging for the diagnosis of bone metastases. Q J Nucl Med, 2001, 45(1):53–64.

[28] Lee CS, Jung CH. Metastatic spinal tumor. Asian Spine J, 2012, 6(1):71–87.

[29] Kumar R, Guinto FC Jr, Madewell JE, David R, Shirkhoda A. Expansile bone lesions of the vertebra. Radiographics, 1988, 8(4):749–769.

[30] Tosi P. Diagnosis and treatment of bone disease in multiple myeloma: spotlight on spinal involvement. Scientifica (Cairo), 2013, 2013:104546.

[31] Kim YS, Han IH, Lee IS, Lee JS, Choi BK. Imaging findings of solitary spinal bony lesions and the differential diagnosis of benign and malignant lesions. J Korean Neurosurg Soc, 2012, 52(2):126–132.

[32] Shah LM, Salzman KL. Imaging of spinal metastatic disease. Int J Surg Oncol, 2011, 2011:769753.

[33] Algra PR, Heimans JJ, Valk J, Nauta JJ, Lachniet M, Van Kooten B. Do metastases in vertebrae begin in the body or the pedicles? Imaging study in 45 patients. AJR Am J Roentgenol, 1992, 158(6):1275–1279.

[34] Jacobson HG, Poppel MH, Shapiro JH, Grossberger S. The vertebral pedicle sign: a Roentgen finding to differentiate metastatic carcinoma from multiple myeloma. Am J Roentgenol Radium Ther Nucl Med, 1958, 80(5):817–821.

[35] Maccauro G, Spinelli MS, Mauro S, Perisano C, Graci C, Rosa MA. Physiopathology of spine metastasis. Int J Surg Oncol, 2011, 2011:107969.

[36] Trilling GM, Cho H, Ugas MA, Saeed S, Katunda A, Jerjes W, Giannoudis P. Spinal metastasis in head and neck cancer. Head Neck Oncol, 2012, 4:36.

[37] Roodman GD. Mechanisms of bone metastasis. N Engl J Med, 2004, 350(16):1655–1664.

[38] Coleman RE. Skeletal complications of malignancy. Cancer, 1997, 80(8 Suppl):1588–1594.

[39] Healy CF, Murray JG, Eustace SJ, Madewell J, O'Gorman PJ, O'Sullivan P. Multiple myeloma: a review of imaging features and radiological techniques. Bone Marrow Res, 2011, 2011: 583439.

[40] Silva JR Jr, Hayashi D, Yonenaga T, Fukuda K, Genant HK, Lin C, Rahmouni A, Guermazi A. MRI of bone marrow abnormalities in hematological malignancies. Diagn Interv Radiol, 2013, 19(5):393–399.

[41] Rahmouni A, Divine M, Mathieu D, Golli M, Haioun C, Dao T, Anglade MC, Reyes F, Vasile N. MR appearance of multiple myeloma of the spine before and after treatment. AJR Am J Roentgenol, 1993, 160(5):1053–1057.

[42] Moulopoulos LA, Dimopoulos MA. Magnetic resonance imaging of the bone marrow in hematologic malignancies. Blood, 1997, 90(6):2127–2147.
[43] Daffner RH, Lupetin AR, Dash N, Deeb ZL, Sefczek RJ, Schapiro RL. MRI in the detection of malignant infiltration of bone marrow. AJR Am J Roentgenol, 1986, 146(2):353–358.
[44] Frank JA, Ling A, Patronas NJ, Carrasquillo JA, Horvath K, Hickey AM, Dwyer AJ. Detection of malignant bone tumors: MR imaging *vs* scintigraphy. AJR Am J Roentgenol, 1990, 155(5):1043–1048.
[45] Shah LM, Hanrahan CH. MRI of spinal bone marrow: Part I, Techniques and normal age-related appearances. AJR Am J Roentgenol, 2011, 197(6):1298–1308.
[46] Hwang S, Panicek DM. Magnetic resonance imaging of bone marrow in oncology, Part 2. Skeletal Radiol, 2007, 36(11): 1017–1027.
[47] Schweitzer ME, Levine C, Mitchell D, Gannon FH, Gomella LG. Bull's-eyes and halos: useful MR discriminators of osseous metastases. Radiology, 1993, 188(1):249–252.
[48] Uchida N, Sugimura K, Kajitani A, Yoshizako T, Ishida T. MR imaging of vertebral metastases: evaluation of fat saturation imaging. Eur J Radiol, 1993, 17(2):91–94.
[49] An C, Lee YH, Kim S, Cho HW, Suh JS, Song HT. Characteristic MRI findings of spinal metastases from various primary cancers: retrospective study of pathologically-confirmed cases. J Korean Soc Magn Reson Med, 2013, 17(1):8–18.
[50] Porter BA, Shields AF, Olson DO. Magnetic resonance imaging of bone marrow disorders. Radiol Clin North Am, 1986, 24(2): 269–289.
[51] Shields AF, Porter BA, Churchley S, Olson DO, Appelbaum FR, Thomas ED. The detection of bone marrow involvement by lymphoma using magnetic resonance imaging. J Clin Oncol, 1987, 5(2):225–230.
[52] Hayes CW, Conway WF, Daniel WW. MR imaging of bone marrow edema pattern: transient osteoporosis, transient bone marrow edema syndrome, or osteonecrosis. Radiographics, 1993, 13(5):1001–1011; discussion 1012.
[53] Daldrup-Link HE, Henning T, Link TM. MR imaging of therapy-induced changes of bone marrow. Eur Radiol, 2007, 17(3): 743–761.
[54] Frank JA, Dwyer AJ, Doppman JL. Magnetic resonance imaging in oncology. In: DeVita VT, Hellman S, Rosenberg SA (eds). Important advances in oncology. Lippincott Williams & Wilkins, Philadelphia, 1987, 133–174.
[55] Linden A, Zankovich R, Theissen P, Diehl V, Schicha H. Malignant lymphoma: bone marrow imaging *versus* biopsy. Radiology, 1989, 173(2):335–339.
[56] Döhner H, Gückel F, Knauf W, Semmler W, van Kaick G, Ho AD, Hunstein W. Magnetic resonance imaging of bone marrow in lymphoproliferative disorders: correlation with bone marrow biopsy. Br J Haematol, 1989, 73(1):12–17.
[57] Dwyer AJ, Frank JA, Sank VJ, Reinig JW, Hickey AM, Doppman JL. Short-Ti inversion-recovery pulse sequence: analysis and initial experience in cancer imaging. Radiology, 1988, 168(3):827–836.
[58] James SLJ, Panicek DM, Davies AM. Bone marrow oedema associated with benign and malignant bone tumours. Eur J Rad, 2008, 67(1):11–21.
[59] Starr AM, Wessely MA, Albastaki U, Pierre-Jerome C, Kettner NW. Bone marrow edema: pathophysiology, differential diagnosis, and imaging. Acta Radiol, 2008, 49(7):771–786.
[60] Bhandari V, Jain RK. A retrospective study of incidence of bone metastasis in head and neck cancer. J Cancer Res Ther, 2013, 9(1):90–93.
[61] Khaw FM, Worthy SA, Gibson MJ, Gholkar A. The appearance on MRI of vertebrae in acute compression of the spinal cord due to metastases. J Bone Joint Surg Br, 1999, 81(5):830–834.
[62] Daldrup-Link HE, Franzius C, Link TM, Laukamp D, Sciuk J, Jürgens H, Schober O, Rummeny EJ. Whole-body MR imaging for detection of bone metastases in children and young adults: comparison with skeletal scintigraphy and FDG PET. AJR Am J Roentgenol, 2001, 177(1):229–236.

Corresponding author
Iulia Alecsandra Sălcianu, MD, PhD, Department of Radiology and Medical Imaging, "Colţea" Clinical Hospital, 1 Ion C. Brătianu Avenue, 030171 Bucharest, Romania; Phone +4021–387 41 00, Fax +4021–387 41 01, e-mail: salcianu_iulia@yahoo.com

Received: October 15, 2016

Accepted: March 7, 2018